PEOPLE'S DEMOCRATIC REPUBLIC OF ALGERIA

MINISTRY OF HIGHER EDUCATION

AND SCIENTIFIC RESEARCH

UNIVERSITY OF SAIDA Dr. MOULAY TAHAR

FACULTY OF SCIENCE

DEPARTMENT OF PHYSICS

DISSERTATION

Submitted in partial fulfillment of the requirements for the degree of

MASTER

In physics of condensed matter

By

SADOUKI Ouafaa

On the subject:

Structural, elastic, electronic and magnetic properties of the quaternary Heusler alloy: CrCoScAl

Defended on 06/09/2020 in front of the jury composed of:

ELKEURTI Mohammed	Chair	Professor	U .Saida
KHELFAOUI Friha	Supervisor	M.C. B	U. Saida
ZEMOULI Mostefa	Examiner	M. C. A	U. Saida

Academic year 2019-2020

Dedication

This work is dedicated:

To my beloved mother and father whose support, encouragement and constant love have sustained me throughout.

To my brothers Sofian, Nouh, Ayoub, Abdelrahman, and my sister in law;

ToAll my relatives and friends;

and finally to you, dearest reader.

SadoukiOuafaa**.**

Acknowledgments

This dissertation marks the end of an arduous, but an insightful journey in scientific research. It would have never been completed without constant support and encouragement from my supervisor, Dr KHELFAOUI Friha, her wisdom, patience, stimulating suggestions and encouragement gave me the energy to complete what at times seemed to be an unattainable goal. I would like to thank her for her invaluable advice and guidance throughout the course of this study.

My sincere thanks and gratitude go to the members of the board of examiners Prof. ELKEURTI Mohammed and Dr ZAMOULI Mostefa, for accepting to read and evaluate this dissertation.

My deepest thanks go to all my friends who have constantly given me support and strength to continue this research and are extended to my colleagues who never refused to assist me. I would like to express my great pride to my beloved parents, brothers for their endless love, sacrifice and support in order to finish this study.

Table of contents

List of figures

List of tables

General introduction

General introduction:

The development of Technology and industry depends on the search for new materials and alloys from the periodic table based on the natural law which states that the combination of two different materials does not present a combination of their properties but instead gives rise to new characteristics specific to the alloy[1]. Recently, Heusler alloys have attracted considerable experimental and theoretical interest due to three unique properties that they exhibit: i) Half-metallic behavior, ii) magnetic shape memory effect and iii) inverse magneto-caloric effect.

The discovery of Heusler alloys dates back to 1903 when the German physicist Friedrich Heusler reported that the addition of sp elements (Al, In, Sn, Sb or Bi) turn Cu-Mn alloy into a ferromagnetic material, even though the alloy contains none of the ferromagnetic elements.[2]. After complete understanding of crystal structure, numerous investigations were made. It is found that two classes of materials are called Heusler alloys: The half-Heusler alloys with general formula XYZ and the full-Heusler alloys with the formula X_2 YZ. However, at the present time in such materials, we can observe not only ferromagnetism, but also antiferromagnetism, paramagnetism, diamagnetism.

The half-metallicity was first predicted by Groot and his collaborators in 1983 when studying the band structure of a half-Heusler alloy NiMnSb[3]. According to this prediction, NiMnSb compound was half-metal material. While one band of half metallic materials, exhibits semiconducting qualities, the other band exhibits metallic properties [4, 5]. Half-metallic ferromagnets have attracted a great deal of interest in spintronic applications in recent years due to the increased application areas. The magnetic sensors [6, 7], tunnel junction and spin-injector materials can be given as examples of these applications of semi-conductor materials [8]. It has also been observed that half-metallic materials reduce electricity consumption and integration intensities [9].

Thus, the objective of the present work is to systemically study the structural, electronic and magnetic properties of the quaternary heusler compound CrCoScAl, using the full-potential linear-augmented plane-wave method (FP-LAPW) in the framework of the density functional theory (DFT) using the generalized gradient approximation of Perdew-Burke-Ernzerhof (GGA-PBE). Whilethe basic introduction of the overview of the

problem undertook, Heusler alloys and the method used constitute Chapter 1 to 3 and the results of the investigations have been discussed in Chapter 4.

Chapter I

Density Functional Theory (DFT)

I.1. Introduction:

Density functional theory is one of the most popular and successful quantum mechanical approaches to matter. It is a method in quantum mechanical modeling that studies the behavior of the material by solving the Schrödinger equation (SE) and finding the ground state of the system. The main idea of DFT is to describe a many-body interacting system via its particle density and not via its many-body wavefunction. Its significance is to reduce the 3N degrees of freedom of the N-body system to only three spatial coordinates through its particle density. It is used to calculate properties such as equilibrium geometries, electronic, optic, activation energies, and reaction energies. The theory originates from the pioneering work due to Thomas[10] and Fermi [11]in the early thirties of the twentieth century and furtherrefinements by Hartree[12], Dirac [13, 14], Fock[15]and Slater .It was given a firm foundation by Hohenberg, Kohn and Sham almost forty years after the work of Thomas and Fermi.In this chapter, we will discuss the general theory and historical background about DFT, as well as, we will introduce some important concepts in DFT.

I.2. Many-body system:

The dynamic of a quantum system is governed by the Hamiltonian$\hat{H}$. If$|\Psi\rangle$ is a quantum state of the system in an abstract Hilbert space representation, its time-evolution is given by:

$$i\hbar\frac{\partial\Psi}{\partial t} = \hat{H}\Psi \tag{I.1}$$

Stationary states with definite energies, particularly the ground state of the system, are obtained as solutions of the eigenvalue equation:

$$\hat{H}|\Psi\rangle = E|\Psi\rangle \quad , \langle\Psi|\Psi\rangle = 1 \tag{I.2}$$

Alternatively, they are obtained as stationary solutions of the variational problem

$$\frac{\langle\Psi|\hat{H}|\Psi\rangle}{\langle\Psi|\Psi\rangle} \rightleftarrows \ stationary \tag{I.3}$$

We are interested in systems of N electrons, M nucleus moving in a given external field and interacting with each other with pair forces, the total wavefunction of the system in this case:

$$\psi = \psi(\vec{r}_1, \vec{r}_2, \dots \vec{r}_N; \vec{R}_1, \vec{R}_2, \dots, \vec{R}_M) \quad \text{(I.4)}$$

And the Hamiltonian consists of:

$$\hat{H} = \hat{T}_N + \hat{T}_e + \hat{V}_{N-N} + \hat{V}_{N-e} + \hat{V}_{e-e} \quad \text{(I.5)}$$

Where:

$\hat{T}_N = -\sum_{I=1}^{M} \frac{\hbar^2}{2M_I} \nabla_I{}^2$: Thekinetic energy of nuclei

$\hat{T}_e = -\sum_{i=1}^{N} \frac{\hbar^2}{2m_e} \nabla_i{}^2$:Thekinetic energy of electrons

$\hat{V}_{N-N} = \frac{1}{2} \sum_{I \neq J} \frac{e^2}{4\pi\varepsilon_0} \frac{Z_I Z_J}{|\vec{R}_I - \vec{R}_J|}$:The potential energy of nucleus-nucleus coulomb interaction

$\hat{V}_{N-e} = \frac{1}{2} \sum_{i,J} \frac{e^2}{4\pi\varepsilon_0} \frac{Z_I}{|\vec{r}_i - \vec{R}_J|}$:Potential energy of nucleus-electron coulomb interaction

$\hat{V}_{e-e} = \frac{1}{2} \sum_{i \neq j} \frac{e^2}{4\pi\varepsilon_0} \frac{1}{|\vec{r}_i - \vec{r}_j|}$:Potential energy of electron-electron coulomb interaction

The wave function contains in principle, all information about a given system[16] . For the case of a simple 2-D square potential or even a hydrogen atom we can solve the Schrödinger equation exactly. Unfortunately, it is impossible for a N-body system. Therefore, we must involve some approximations to make the problem soluble.

I.2.1. Born-Oppenheimer approximation:

A so-called Born Oppenheimer (BO) approximation was made by Born and Oppenheimer [17]in 1927. Since the nuclei are much heavier than electrons (the mass of a proton is about 1836 times the mass of an electron), the nuclei move much slower (about two order of magnitude slower) than the electrons.Therefore, we can separate the movement of nuclei and electrons that's why it's called adiabatic. When we consider the movement of electrons, it is reasonable to consider the positions of nuclei are fixed,thusThe Hamiltonian can be written as:

$$\hat{H}_e = \hat{T}_e + \hat{V}_{N-e} + \hat{V}_{e-e} \quad \text{(I.6)}$$

The total wave function can be written as:

$$\psi(\vec{R}_I, \vec{r}_i) = \varphi_N(\vec{R}_I)\psi_e(\vec{R}_I, \vec{r}_i) \quad \text{(I.7)}$$

where$\varphi_N(\vec{R}_I)$ describes the nuclei and $\psi_e(\vec{R}_I, \vec{r}_i)$ describe the electrons (depending parametrically on the positions of the nuclei).With the BO approximation, The Schrödinger equation for electrons is written:

$$\hat{H}_e\psi_e = E_e\psi_e \quad \text{(I.8)}$$

This approximation has reduced the degree of complexity of the problem, but still unresolved because for a system with N electrons, it depends on 3N space coordinates and N spin coordinates.

I.2.2. Hartree approximation:

The complexity of solving equation (I.8) is due to electron-electron interactions, which prevents the separation of this equation into n electronic equations. In the Hartree approximation [12], We consider the electrons as independent, in which each electron moves in a middle field created by nuclei and other electrons.

The Hamiltonian can be written:

$$\hat{H}_e = \sum_i h_i \quad \text{(I.9)}$$

whereh_i is : the mono electronic hamiltonian.

$$h_i = -\frac{\hbar^2}{2m_e}\nabla_i{}^2 + \hat{V}_{ext}(\vec{r}) + \hat{V}_i(\vec{r}) \quad \text{(I.10)}$$

With$\hat{V}_i(\vec{r}) = \int \frac{\rho(\vec{r}')}{|\vec{r}-\vec{r}'|} d^3\vec{r}'$: the Hartree potential

$\hat{V}_{ext}(\vec{r})$:the Coulomb interaction of the electron with all the nuclei of the system

The electronic wave function of this Hamiltonian is a product of mono-electronic functions (Hartree Product (HP)

$$\psi_e(\vec{r}_1, \vec{r}_2, \ldots\ldots, \overrightarrow{r_N}) = \phi_1(\vec{r}_1) \ldots\ldots \phi_N(\vec{r}_N) \quad \text{(I.11)}$$

In this case, each of these mono-electronic wave function is then a solution of the Schrödinger equation to a particle which is written in the form:

$$h_i(\vec{r})\phi_i(\vec{r}) = \varepsilon_i\phi_i(\vec{r}) \tag{I.12}$$

The wave function represented by **equation (I.11)** is not yet complete because it does not respect Pauli's exclusion principle which states that, since electrons are "fermions", the wave function must change sign if we exchange the variables of two electrons, This principle is equivalent to the statement that two electrons cannot occupy the same electronic state[18] The antisymmetric wave function must check:

$$\psi_e\left(\vec{r}_1, \vec{r}_2 \dots \vec{r}_i, \vec{r}_j \dots \vec{r}_N\right) = -\psi_e\left(\vec{r}_1, \vec{r}_2 \dots \vec{r}_j, \vec{r}_i \dots \vec{r}_N\right) \tag{I.13}$$

I.2.3. HartreeFock approximation:

In 1930, Fock[15] showed that the equations of Hartree neglect a very important concept which is the antisymmetric form of the total wave function that must be put by construction in the form of Slater's determine,thus the mono-electronic wave function can be written :

$$\psi(\vec{r}_1, \vec{r}_2, \dots \dots \dots, \overrightarrow{r_N}) = \frac{1}{\sqrt{N!}}\begin{vmatrix} \phi_1(\vec{r}_1)\phi_1(\overrightarrow{r_2}) \dots \phi_1(\vec{r}_N) \\ \phi_2(\vec{r}_1)\phi_2(\overrightarrow{r_2}) \dots \phi_1(\vec{r}_N) \\ . \quad . \quad . \\ . \quad . \quad . \\ \phi_N(\vec{r}_1)\phi_N(\overrightarrow{r_2}) \dots \phi_1(\vec{r}_N) \end{vmatrix} \tag{I.14}$$

This is the easiest way to respect the Pauli's exclusion principle. The mono-electronic equations are written:

$$\left[-\frac{\nabla^2}{2} + \hat{V}_{ext}(\vec{r}) + \hat{V}_i(\vec{r})\right]\phi_i(\vec{r}) + \int d\vec{r}' V_X(\vec{r}, \vec{r}')\phi_i(\vec{r}') = \varepsilon_i\phi_i(\vec{r}) \tag{I.15}$$

By simplifying the equation:

$$h_i\phi_i(\vec{r}) + \int d\vec{r}' V_X(\vec{r}, \vec{r}')\phi_i(\vec{r}') = \varepsilon_i\phi_i(\vec{r}) \tag{I.16}$$

With

$V_X(\vec{r}, \vec{r}') = -\sum_j \frac{\phi_j{}^*(\vec{r}')\phi_j(\vec{r})}{|\vec{r}-\vec{r}'|}$: The HartreeFock exchange potential

Physically, the V_X potential flows precisely from the Pauli Exclusion Principle, and prevents two electrons from occupying the same quantum state. This set of equations

is self-consistent (via the term Hartree and the non-local term Fock). The evaluation of the potential $V_X$implies an integration on the additional variable r'Which complicates enormously the practical solution of Hartree-Fock equations[19] . The calculation is very heavy from a numerical point

of view. This is why the density functional method is often used because it dramatically and surprisingly simplifies calculations.

I.3. Density functional theory:

The basic concept of density functional theory is to use the electron density as the fundamental variable, unlike Hartree-Fock theory which deals directly with the wavefunctionof the electrons. Using the electron density significantly speeds up the calculation. Whereas the electronic wavefunction is a function of 3N variables (the coordinates of all N atoms in the system).while, the electron density is a function of only three variables (x, y, z). Therefore we need to be sure that we can derive something significant from it. It was Hohenburg and Kohn, who stated a theorem which tells us that the electron density is very useful. From that time on, density functional theory has grown vastly in popularity, and a flood of computational work in molecular and solid state physics has been the result. Before addressing the foundations of the Density functional Theory, it seems essential to define the electron density.

I.3.1. Electron density:

An electron cannot be localized as an individual particle [20], but its probability of presence in an element of volume $d^3\vec{r}$ can be estimated and corresponds to the electronic density $\rho(\vec{r})$

$$\psi(\vec{r}) = \sum_{i=1}^{N} |\varphi_i(\vec{r})|^2 \qquad \text{(I.17)}$$

This guarantees that $\rho(\vec{r})$will always have a positive value (positive function), and this value expresses the relative probability of finding an electron at a particular location. This function has lots of properties:

$* \int \rho(\vec{r}) d\vec{r} = N$ (Integration over the entire space), while N is total number of electrons

*$\rho(\mathrm{r}=\infty)=0$

* $\rho(\vec{r})$is an observable that can be measured experimentally (by X-ray diffraction)

All of these arguments seem to indicate that the electronic density is sufficient to have a complete determination of the properties of an atomic system.

I.3.2. Hohenberg-Kohn (HK) theorems:

DFT is made possible by the existence of two ingeniously simple theorems put forward and proven by Hohenberg and Kohn in 1964[21].

a. Theorem I

For any system of interacting particles in an external potential $V_{ext}(\vec{r}_i)$, the density is uniquely determined (in other words, the external potential is a unique functional of the density).

Proof:

Suppose there are two different external potentials$V_{ext}(\vec{r}_i)$and $V'_{ext}(\vec{r}_i)$ which differ by more than a constant and lead to the same ground state density $\rho_0(r)$. Obviously $V_{ext}(\vec{r}_i)$and $V'_{ext}(\vec{r}_i)$ belong to distinct Hamiltonians $\hat{H}$ and $\widehat{H'}$ which give rise to distinct wavefunctions$\Psi$and $\Psi'$with $\hat{H}\Psi = E_0\Psi$ and $\hat{H}'\Psi' = E'_0\Psi'$. Since Ψ' is not the ground state of $\hat{H}$,it follows that :

$$E_0 < \langle\Psi'|\hat{H}|\Psi'\rangle \tag{I.18}$$

$$< \langle\Psi'|\widehat{H'}|\Psi'\rangle + \langle\Psi'|\hat{H} - \widehat{H'}|\Psi'\rangle \tag{I.19}$$

$$< E'_0 + \int \rho_0(r)[V_{ext}(\vec{r}_i) - V'_{ext}(\vec{r}_i)]\overrightarrow{dr} \tag{I.20}$$

Similarly

$$E'_0 < \langle\Psi|\widehat{H'}|\Psi\rangle \tag{I.21}$$

$$< \langle\Psi|\widehat{H'}|\Psi\rangle + \langle\Psi|\widehat{H'} - \hat{H}|\Psi\rangle \tag{I.22}$$

$$< E_0 + \int \rho_0(r)[V'_{ext}(\vec{r}_i) - V_{ext}(\vec{r}_i)]\overrightarrow{dr} \tag{I.23}$$

Adding **Equations(I.20)**and **(I.23)** lead to the contradiction

$$E_0 + E'_0 < E'_0 + E_0 \quad \text{(I.24)}$$

Hence, no two different external potentials $V_{ext}(\vec{r}_i)$ can give rise to the same ground state density$\rho_0(\vec{r})$, the ground state density determines the external potential. $V_{ext}(\vec{r})$, except for a constant.That is to say, the base variable is no longer necessarily the wave function; the basic variable is now the electronic density which completely describes the ground state and all its properties, this leads to the formulation of the second theorem ofHohenberget Kohn.

b. Theorem II :

A universal functional for the energy E[ρ] can be defined in terms of the density. The exact ground state is the global minimum value of this functional.

Proof:

Since the external potential is uniquely determined by the density and since the potential in turn uniquely (except in degenerate situations) determines the ground state wavefunction, all the other observables of the system such as kinetic energy are uniquely determined. Then one may write the energy as a functional of the density

The functional$E\ [\rho(\vec{r})]$can be written as :

$$E[\rho(\vec{r})] = [\hat{T}] + \left[\hat{V}_{int}\right] + \int V_{ext}\ (\rho(\vec{r}))\overrightarrow{dr} \quad \text{(I.25)}$$

$$= F[\rho(\vec{r})] + \int V_{ext}\ (\rho(\vec{r}))\overrightarrow{dr} \quad \text{(I.26)}$$

where

$F[\rho(\vec{r})]$is a universal functional

In the ground state the energy is defined by the unique ground state density $\rho_0(\vec{r})$

$$E_0 = E[\rho_0(\vec{r})] = \langle \Psi | \hat{H} | \Psi \rangle \quad \text{(I.27)}$$

By the variational principle, a different density$\rho'(\vec{r})$ will necessarily give a higher energy

$$E_0 = \langle \Psi | \hat{H} | \Psi \rangle < \langle \Psi' | \hat{H} | \Psi' \rangle = E' \quad \text{(I.28)}$$

It follows that minimizing with respect to $\rho(\vec{r})$, the total energy of the system written as a functional of $\rho(\vec{r})$. One finds the total energy of the ground state, the correct density that minimizes the energy is then the ground state density.

Notice that There is no exact formulation for expressing the kinetic energy as a functional of electronic density,the equations of Khon and Sham [22] present the only solution to this problem.

I.3.3. Kohn-Sham equation:

Kohn-Sham (KS) equationput Hohenberg-Kohn theorems into practical use and makes DFT calculations possible with even a single personal computer[23]. It was so successful that Kohn was honored the Nobel prize in chemistry in 1998.The KS equation maps the original interacting system with real potential V_{ext} into a fictitious non-interacting system with an effective potential V_{eff} and assume that the two systems have exactly the same ground state density.As mentioned above in **equation (I.28)**, The expressions of T and V_{int} were not known, Kohn and Sham proposed the next separations:

$$T[\rho(\vec{r})] = T_0[\rho(\vec{r})] + (T[\rho(\vec{r})] - T_0[\rho(\vec{r})]) \quad \text{(I.29)}$$

$$= T_0[\rho(\vec{r})] + E_c[\rho(\vec{r})] \quad \text{(I.30)}$$

Where

$T_0[\rho(\vec{r})]$: The kinetic energy of non-interacting electron gas.

$E_c[\rho(\vec{r})]$: the correlation energy that is neglected in the Hartree-Fock approximation.

$$V_{int}[\rho(\vec{r})] = E_H[\rho(\vec{r})] + (V_{int}[\rho(\vec{r})] - E_H[\rho(\vec{r})]) \quad \text{(I.31)}$$

$$= E_H[\rho(\vec{r})] + E_x[\rho(\vec{r})] \quad \text{(I.32)}$$

Where

$E_H[\rho(\vec{r})]$: Term of Hartree.

$E_x[\rho(\vec{r})]$: Exchange energy that is neglected by Hartree.

Then

$$F[\rho(\vec{r})]=T_0[\rho(\vec{r})]+E_c[\rho(\vec{r})]+E_H[\rho(\vec{r})]+E_x[\rho(\vec{r})] \quad \text{(I.33)}$$

$$F[\rho(\vec{r})]=T_0[\rho(\vec{r})]+E_H[\rho(\vec{r})]+E_{xc}[\rho(\vec{r})] \quad \text{(I.34)}$$

Therefore, the functional energy of Hohenberg and Kohn can be expressed by the following equation:

$$E[\rho(\vec{r})]=T_0[\rho(\vec{r})]+E_H[\rho(\vec{r})]+E_{xc}[\rho(\vec{r})]+\int \rho(\vec{r})V_{ext}(\vec{r})d\vec{r} \quad \text{(I.35)}$$

With $E_{XC}[\rho(\vec{r})]$: Exchange-correlation energy,is due to the difference between the non-interacting and the interacting kinetic energies and also to the difference between real interaction energy and that of Hartree. The equations of Kohn and Sham that solve the problem is :

$$\left[-\frac{h^2}{2m_e}\vec{\nabla}_i^2+V_{eff}(\vec{r})\right]\varphi_i(\vec{r})=\varepsilon_i\varphi_i(\vec{r}) \quad \text{,i=1,……N} \quad \text{(I.36)}$$

Where there is one electron in each of the N orbitals $\varphi_i(\vec{r})$, with the lowest eigenvaluesε_i.

The density of the auxiliary system is constructed from:

$$\rho(\vec{r})=\sum_{i=1}^{N}|\varphi_i(\vec{r})|^2 \quad \text{(I.37)}$$

The effective potential is of the form:

$$V_{eff}(\vec{r})=V_{ext}[\rho(\vec{r})]+V_H[\rho(\vec{r})]+V_{xc}[\rho(\vec{r})] \quad \text{(I.38)}$$

With

$$V_H[\rho(\vec{r})]=\frac{1}{2}\int\frac{e^2}{4\pi\varepsilon_0}\frac{\rho(\vec{r}')}{|\vec{r}-\vec{r}'|}d^3\vec{r}' : \text{Hartree potential}$$

$$V_{xc}[\rho(\vec{r})] = \frac{\delta E_{xc}[\rho(\vec{r})]}{\delta\rho(\vec{r})} : \text{Exchange} - \text{correlation potential}$$

Until now the DFT is an exact method, but to become more usable in practice, we need to propose a formulation of $E_{xc}[\rho(\vec{r})]$ and for that we are obliged to to go through an approximation.

I.3.4. Solving kohn-sham equations

By using independent-particle methods, the KS equations provide a way to obtain the exact density and energy of the ground state of a condensed matter system. The KS equations must be solved consistently because the effective KS potential $V_{eff}(\vec{r})$ and the electron density $\rho(\vec{r})$ are closely related. This is usually done numerically through some self-consistent iteration as shown in**Figure (II.2).**

Finding a suitable solution can be accomplished by following these steps:

1. Start with an initial electron density for the first iteration.
2. Calculation of the effective KS.
3. Resolution of the Kohn-Sham equation with single particle eigenvalues and wavefunctions.
4. Calculation of the new electron density from the wavefunctions.
5. Examination of self-consistent condition(s) (by comparing the old and the new densities).
6. Calculation of the different physical quantities (Energy, forces, ...); End of calculation.

Chapter II

Methodology

II.1. Introduction:

In this chapter, we are going to present the methodology used in the calculation of our work. We explain how the exchange-potential correlation can be treated through various approximations (LDA,LSDA, GGA and LDA+U). We attempt to introduce the fundamental concepts of the linearized / augmented plane wave plus local orbitals (L/APW+lo). We show also the different versions of (L/APW+lo) and their main developing steps in terms of linearization, full potential, local orbitals and mixed basis sets. Then, we will submit the wien2k code.

II.2. Augmented Plane Wave methods:

To determine the electronic, optical, thermal, mechanical or magneticproperties of materials, several different methods of calculating have been developed andthey are classified into three categories according to the used data.

- ✓ Empirical methods: consist of the using of the experience to find the values of the parameters hence the empirical result is a unified confirmation.
- ✓ Semi empirical methods:require pre-calculated data and the experimental results to predict other properties that are not yet determined experimentally.This method speeds up calculation to such an extent that even large molecules can be calculated.
- ✓ Ab-initio methods: for which calculations require only basic data.

In the recent years, researchers have developed ab-initio methods with no inclusion of experimental data,based on theoretical principles,known as "first principles methods"one of the most widely used methodis : Full Potential Linearized Augmented Plane Wave (FP-LAPW)developed by Andersen [24]which is just an amelioration of another approximation called augmented plane wave (APW).

II.2.1. APW method:

APW method is one of the most popular techniques for the solution of the electronic,structureusing Kohn-Sham (KS) equations. Slater proposed the technique in 1937[19, 25] .He supposed that in the region far away from the nuclei, the electrons are more or less free, free electrons are described by plane waves. Close to the nuclei, the electrons behave quite as they were in a free atom, and they could be described

more efficiently by atomic like functions. Space is therefore divided now in two regions: around each atom a sphere with radius R_α is drawn (call itS_α). Such a sphere is often called a muffin tin sphere[19] the part of space occupied by the spheres is the muffin tin region. The remaining space outside the spheres is called the interstitial region (call it I). One augmented plane wave (APW) used in the expansion of is defined as:

$$\phi(\vec{r}) = \begin{cases} \varphi_i(\vec{r}) = \frac{1}{\Omega^{\frac{1}{2}}} \sum_G C_G \, e^{i(\vec{k}+\vec{G})\vec{r}} r > R_\alpha \\ \varphi_s(\vec{r}) = \sum_{lm} A_{lm} U_l^\alpha(r, E_l) Y_{lm}(\vec{r}) \, r < R_\alpha \end{cases} \quad \text{(II.1)}$$

From (II.1) φ is the wave function, Ω is the unit cell volume, C_G and A_{lm} are expansion coefficients , $Y_{l,m}$ are spherical harmonics ;U_l^α is the numerical solution to the radialSchrödinger equation which is given by:

$$\left\{-\frac{d^2}{dr^2} + \frac{l(l+1)}{r^2} + V(r) - E_{nl}\right\} r U_l(r) = 0 \quad \text{(II.2)}$$

Slater has motivated the use of these functions by noting that plane waves are the solutions of the Schrödinger's equation in a constant potential and radial functions are solutions in a spherical potential.Since the continuity on the spheres boundaries needs to be guaranteed on the dual representation defined in **equation (II.1)**, constraint must be imposed. In the APW method, this is done by defining the U_l^α in terms of C_G in the spherical harmonic expansion of the plane waves

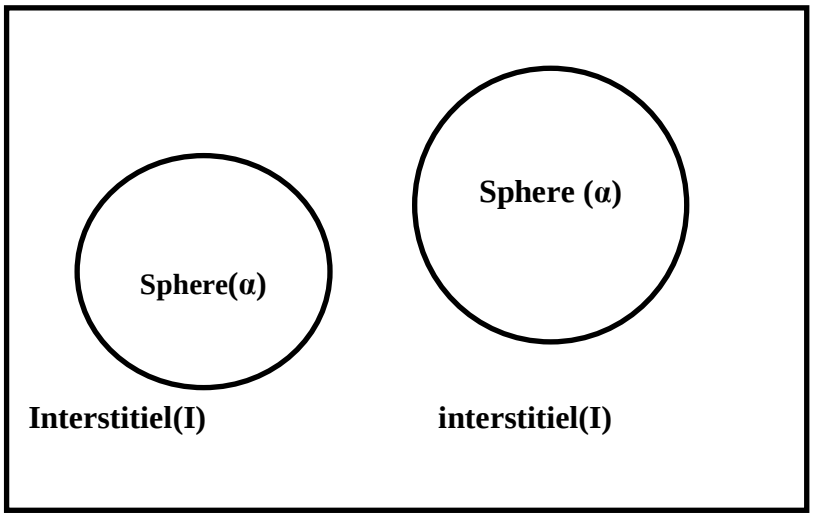

Figure II.1: Adaptation of the basis set by dividing the unit cell intoatomic spheres and interstitial regions.

In the APW technique, continues basis sets (functions) are used, which cover all the space within the sphere. However, APW is a commonly used technique for the calculations of the structural, electronic, optical and magnetic properties of solids but even then, it has some disadvantages. One example of the limitation of this technique is; it cannot be extended beyond the average spherical muffin-tin approximation. The basic functions, for this approach, have a kink at the border of the muffin-tin and hence at the boundary their derivatives are discontinues. Another drawback of this approach is the radial function$U_l^\alpha(r, E_l)$is dependent upon energy, which leads a nonlinear eigenvalue problem. This can cause numerical complications ifU_l^αbecome very small at the empty sphere boundary. Therefore, in order to overcome this problem, several modifications to the APW method have been made, notably those proposed by Koelling[26] and Andersen [27]

II.2.2. LAPW method:

To avoid the problems connected with the APW method resulting from the discontinuity of the basis functions and their first derivative at the muffin-tin boundary between core and interstitial region, in the middle of the seventies linearized methods were invented by Andersen[27] and Koelling and Arbman[26] . Based on an idea proposed by Marcus. To solve the problem Anderson launched an additional term in the basis within the MT sphere. In the LAPW technique inside the MT region, the radial wave function is linearized by a linear combination of $U_l(r, E_l)$and $\dot{U}_l(r, E_l)$

$$\phi(\vec{r}) = \begin{cases} \varphi_i(\vec{r}) = \frac{1}{\Omega^{\frac{1}{2}}} \sum_G C_G \, e^{i(\vec{k}+\vec{G})\vec{r}} \, r > R \\ \varphi_s(\vec{r}) = \sum_{lm} \left[A_{lm} U_l(r, E_0) + B_{lm} \dot{U}_l(r, E_0)\right] Y_{lm}(\vec{r}) \, r < R \end{cases} \quad \text{(II.3)}$$

where the B_{lm} coefficients for the energy derivative analogous to theA_{lm}.The basis functions inside the spheres are linear combinations of a radial functions $U_l(r)Y_{lm}(\vec{r})$and their energy derivatives $\dot{U}_l(r)Y_{lm}(\vec{r})$ are the augmenting functions. The U_l are defined as in the APW method **equation (II.1)** and the energy derivative, $\dot{U}_l(r)Y_{lm}(\vec{r})$, satisfies the following equation:

$$\left\{-\frac{d^2}{dr^2} + \frac{l(l+1)}{r^2} + V(r) - E_l\right\} r\dot{U}_l(r) = 0 \quad \text{(II.4)}$$

In the augmented plane wave method the interstitial regions are treated with plane waves only like APW method,while the Muffin-tin regions are treated with better adapted function then APW functionsthe radial basis-function is thereby replaced by the Taylor series:

$$U_l(r,E) = U_l(r,E_l) + (E-E_0)\dot{U}_l(r-E_0) + O((E-E_l)^2) \quad \text{(II.5)}$$

$$\text{While}\dot{U}_l(r,E_0) = \frac{\partial U_l(r)}{\partial E} \quad \text{(II.6)}$$

In this way, the wavefunctions are affected by an error which is quadratic in the deviation of the eigenvalue E from the energy parameter E_l , the error in the eigenvalues enter only to fourth order,thus The LAPW method ensures the continuity of the wave function on the surface of the MT sphere.

II.2.3. (APW+LO) method:

The APW basis functions can also be modified just like the LAPW ones by introducing local orbitals. Sjosted et al. [28] improved APW by introducing local orbital (lo), APW+lo basis. As in the APW approach, the radial wavefunction is evaluated at fixed energy but this new technique includes another type of orbital's for flexibility. These orbitals are denoted by lo instead of LO in the LAPW [29]

$$\phi(\vec{r}) = \begin{cases} 0 & r > R_\alpha \\ \left[A_{lm}\,U_l(r,E_l) + B_{lm}\,\dot{U}_l(r,E_l)\right]Y_{lm}(\vec{r}) & r < R_\alpha \end{cases} \quad \text{(II.7)}$$

The normalization condition that the function (r) at the MT radii is zero determines the two coefficients in the equation. In this approach $\dot{U}_l$does not depend upon the plane waves and is included only for the selected set of the l quantum numbers. The energy derivative term in the APW+lo, method is only included in just a few lo's and not in every plane wave like that in the LAPW one. Therefore we are not sure that the energyLinearization of APW+lo basis is accurate like LAPW, though it converges faster than LAPW and gives the same accuracy as LAPW technique [26].

II.3. Exchange-potential correlation:

II.3.1. Local density approximation (LDA) :

Kohn and Sham introduced the Local Density Approximation (LDA) in 1965[30]. It is the most widely used one, whichassumes that the density can be treated locally as an uniform electron gas; the exchange correlation energy at each point in the system is the same as that of an uniform electron gas of the same density,and it can be written as :

$$E_{xc}^{LDA}[\rho(\vec{r})] = \int \rho(\vec{r})\, \varepsilon_{xc}^{hom}[\rho(\vec{r})]d^3\vec{r} \quad \text{(II.8)}$$

Where$\varepsilon_{xc}^{hom}[\rho(\vec{r})]$: The exchange-correlation energy per particle. The exchange-correlation potential is then given by:

$$V_{xc}[\rho(\vec{r})] = \frac{\delta E_{xc}[\rho(\vec{r})]}{\delta\rho(\vec{r})} = \varepsilon_{xc}^{hom}[(\vec{r})]+\rho(\vec{r})\frac{\delta\varepsilon_{xc}^{hom}[\rho(\vec{r})]}{\delta\rho(\vec{r})} \quad \text{(II.9)}$$

For practical use of the LDA in calculations it is necessary to determine the exchange-correlation energy for a uniform electron gas of a given density. It is common to split $\varepsilon_{xc}(\rho(\vec{r}))$ into exchange and correlation potentials

$$\varepsilon_{xc}(\rho(\vec{r})) = \varepsilon_x(\rho(\vec{r})) + \varepsilon_c(\rho(\vec{r})) \quad \text{(II.10)}$$

The exchange term, commonly referred to Dirac's exchange[14] (symbolized by S, means that this expression was taken over by Slater)

$$\varepsilon_x^s(\rho(\vec{r}))=-\frac{3}{4}\left(\frac{3\rho(\vec{r})}{\pi}\right)^{1/3} \quad \text{(II.11)}$$

the exactly Accurate values for $\varepsilon_x^s(\rho(\vec{r}))$ have been determined from Quantum Monte Carlo (QMC) calculations[10]These have then been interpolated to provide an analytic form for $\varepsilon_c(\rho(\vec{r}))$.

II.3.2.local spin density approximation (LSDA):

In the case of magnetic materials, the electron spin provides an additional degree of freedom and the LDA must then be extended to the Local Spin Density Approximation (LSDA) where the exchange and correlation energy becomes a functional of the two densities (spin up (↑) and spin down(↓) densities)[31].

$$E_{xc}^{LSDA}[\rho(\vec{r})]=\int \rho(\vec{r})\varepsilon_{xc}^{hom}[(\rho_{\uparrow}(\vec{r}),(\rho_{\downarrow}(\vec{r})]d^3\vec{r} \quad \text{(II.12)}$$

Although it provides good results in many cases, the LDA remains unsuitable for the treatment of transition states and for the calculation of binding energies[32]In order to take into account the inhomogeneity effects of electronic density, generalized gradient approximations (GGA) have been proposed

II.3.3.Generalized gradient approximations (GGA):

As mentioned above, the LDA neglects the inhomogeneity of the real charge density, this leads to the development of various generalized-gradient approximations (GGAs), whichinclude density gradient corrections $\left|\vec{\nabla}\rho(\vec{r})\right|$ and higher spatial derivatives of the electron density $\rho(\vec{r})$ so the correlation energy can be written as :

$$E_{xc}^{GGA}(\rho(\vec{r}))=\int f_{xc}[\rho(\vec{r}),\nabla\rho(\vec{r})]d^3\vec{r} \quad \text{(II.13)}$$

The different GGAs that exist, differ from each other by the choice of the functional f_{xc}.The three most widely used GGAs are the forms proposed by Becke[33], Perdewet al [34], and Perdew, Burke and Enzerhof[35]. GGA generally works better than LDA, in predicting bond length and binding energy of molecules, crystal lattice constants, and so on, especially in systems where the charge density is rapidly varying. However, GGA sometimes overcorrects LDA results in ionic crystals where the lattice constants from LDA calculations fit well with experimental data but GGA will overestimate it. Nevertheless, both LDA and GGA perform badly in materials where the electrons tend to be localized and strongly correlated such as transition metal oxides and rare-earth elements and compounds. This drawback leads to approximations beyond LDA and GGA.

II.3.4. LDA+U Method:

Strongly correlated systems usually contain transition metal or rare earth metal ions with partially filled d or f shells. Because of the orbital-independent potentials in L(S) DA and GGA, they cannot properly describe such systems , In order to properly describe these systems, a modification of the LDA is necessary , which leads us to another approximation called LDA+U(Anisimov, al 1991)[36]To do this, we add Coulomb interaction type Hubbard to the Hamiltonian of Kohn-Sham

$$E_U = \frac{U}{2} \sum_{i \neq j} n_i \, n_j \qquad \text{(II.14)}$$

Where n_i: number of occupied orbitals.

II.4. WIEN2K code:

In the following years significantly improved and updated UNIX-type versions of the original WIEN-code were developed, which were called, according to the year of their publication WIEN93, WIEN95 and WIEN97. Now a new version, WIEN2k, is available, which is based on the full-potential (linearized) augmented plane-wave. This allows a significant improvement, especially in terms of speed, universality, user-friendliness and new features. The WIEN2k is written in FORTRAN 90 and requires a UNIX-type operating system since the programs are linked together via C-shell scripts.It allows to perform electronic structure calculations of solids: electron density, density of states (DOS), various types of spectra, magnetism (ferromagnetic, antiferromagnetic and non-magnetic configurations), non-collinear magnetism, band structure, Fermi surface using density functional theory (DFT). The calculation procedure goes through three stages:

II.4.1. Initialization:

It consists in constructing the spatial configuration (geometry), the operations of symmetry, the starting densities, the number of special points required for integration into the irreducible Brillouin zone ….etc. All these operations are carried out due to a series of auxiliary programs:

Nearest neighbor's distances: This subprogram uses the case.struct file in which the atomic positions in the unit cell are specified, calculates the nearest neighbor distances of all atoms, and checks that the corresponding atomic spheres (radii) are not overlapping. If an overlap occurs, an error message is shown on the screen. In addition, the next nearest-neighbor distance (must be specified interactively) are written to an output file named case.outputnnII**.**

SGROUP: This subprogram uses information from case.struct (lattice type, lattice constants, and atomic positions) to determine the space group as well as all point groups of non-equivalent sites and output the cas.sruct.sgroup file**.**

SYMMETRY: This subprogram uses information from case.struct (lattice type, atomic positions) to list the symmetry operations of the spatial group of the structure and determine the point group of the different atomic locations, and the matrices of the corresponding rotation operations.

LSTAR: It generates atomic densities and determines how the different orbitals will be treated in the band structure calculations. In addition, this program requires the cut-off energy which separates the states of the core from those of valence, usually taken as -6.0Ry[37]

KGEN: The KGEN generates the number of k points in the Brillouin zone.

DSTART: It generates a starting density for the self-coherent cycle by a superposition of atomic densities produced in the START.

II.4.2. Self-consistent calculation (SCF):

The second step is the SCF calculation **Figure (II.2)**. This step consists of the subprograms in cyclic form:

LAPW0: generates the potential for density calculation.

LAPW1: allows the calculation of the valence bands, the eigenvalues and the eigen vectors.

LAPW2: calculates the valence densities for eigenvectors.

LCORE:yields core eigenvalues with the corresponding core densities.

MIXER:the electron densities of core, semi-core, and valence states are added to yield the total density.

II.4.3. Determination of properties:

Once the self-coherent calculation is completed, the properties of the ground state (charge density, band structure, optical properties ... etc.) are then determined.

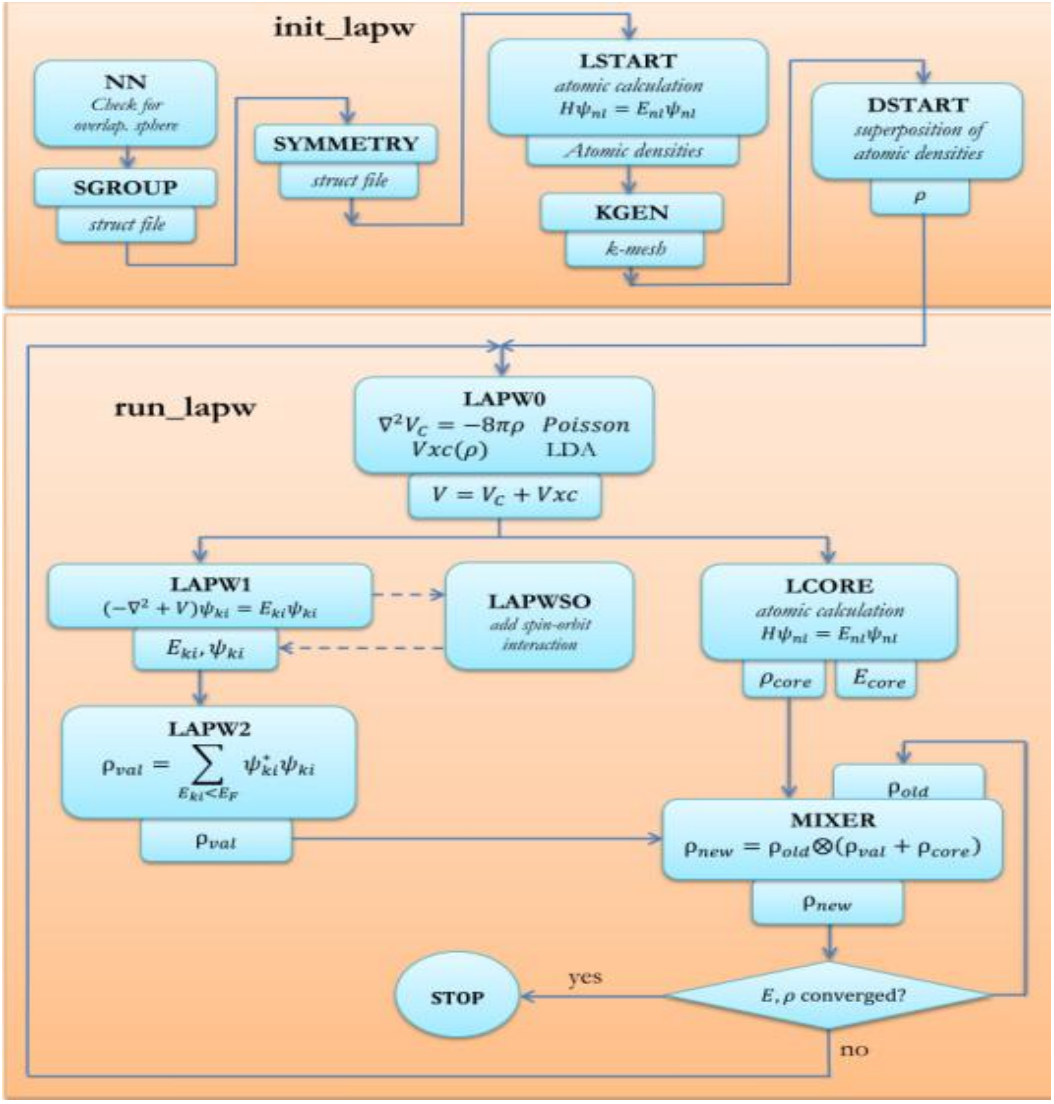

Figure II.2: DFT WIEN2K

Chapter III
Magnetism and Heusler alloys

III.1. Introduction:

At the present time, magnetism in any substances is of great interest. There are five main types of magnetic ordering, associated with the concepts of diamagnetism, paramagnetism, ferromagnetism, antiferromagnetism and ferrimagnetism.The substances, which have a magnetic moment *when*they placed in a magnetic field (magnetization process), are called magnets. Actually absolutely all materials are magnetized to some extentand, hence,can be considered as magnetic and categorized as weak (diamagnets or paramagnets) and strong magnetic(ferromagnets).

Interpretation of magnetic phenomena in solids is based on two basic concepts. The first is that ions in a solid can have discrete magnetic moments. The induced moments are created byexternal magnetic fields. Spontaneous momentsexist evenin the absence of the external fields. The second idea is that these microscopic magnetic moments interact not only as ordinary dipoles (such forces are too weak to play an essential role), but they are also connected by the forces of quantum mechanical nature. So-called exchange forces depend on the distance between the magnetic ions, but also on their mutual geometric arrangement, and cause a variety of types of magnetic ordering in solids[38, 39]

III.2. Magnetization:

The magnetization ***M*** of a small volume of matter is the sum (a vector sum) of the magnetic dipole moments in the small volume divided by that volume. ***M*** is measured in units of amperes per meter.

$$\bar{M}=\frac{1}{V}\sum_{i=1}^{N}\bar{m}_i \qquad \text{(III.1)}$$

The degree of induced magnetization is given by the magnetic susceptibility of the material χ, which is commonly defined by the equation:

$$M=\chi H \qquad \text{(III.2)}$$

Where H is the external magnetic field.The susceptibility is negative for diamagnets and positive for paramagnets. The magnitude of susceptibility for both paramagnets and diamagnets is small, in range $10^{-4}-10^{-6}$. In addition, there are strongly magnetic substances in which the magnetization is not a linear function of the field, ferromagnets, ferrimagnets, antiferromagnets[40].

III.2.1. Paramagnetic materials:

Paramagnets are magnetized in the direction of an external magnetic field, thus having a positive magnetic susceptibility. This is a non-cooperative magnetism, which arises from the presence of spontaneous magnetic moments inions. Paramagnet is misobserved inthe case when the concentration of magnetic atoms or ions in the medium is relatively small and magnetic moments are separated from each other at a distance sufficient to regard them as noninteracting. Diamagnetic and paramagnetic materials are considered non-magnetic because they only have magnetization in the presence of an external field.

III.2.2. Ferromagnetic materials:

Ferromagnetism is a one of the types of magnetism, which can be explained by establishing collinear long-range order of all magnetic moments in the system at temperatures below the Curie point $\boldsymbol{T_c}$. There is then a spontaneous magnetization even in the absence of an applied magnetic field. Ferromagnets are substances with strong magnetic properties. The reason for such strong properties is that the magnetic moments of the atoms are oriented in parallel, which leads to large magnetization called spontaneous magnetization. Note that, above$\boldsymbol{T_c}$ferromagnets behave as paramagnets.In the ideal ferromagnets, all ions have identical spontaneous magnetic moments and they occupy identical crystallographic positions. The ferromagnetism is an example of magnetism, in which the external field plays the role that makes it possible to reveal the existence of microscopic ordering at the macroscopic level[18].

III.2.3. Antiferromagnetic materials:

For the antiferromagnetism, the neighboring spins (two sub lattices) in the magnet are directed in opposite directions and compensate each other. It leads to the absence of spontaneous magnetization and strong magnetism. Therefore, they are classified as weak magnets and their susceptibility have the same order of magnitude as for paramagnets (10^{-5}-10^{-4}). Neighbouring spins in antiferromagnets are oriented antiparallel due to strong interaction, so their stable ordering is preserved up to high temperatures. With such ordering, the strong interaction prevents moment orientation along the applied field. The effect is related to spin structure properties of the antiferromagnet near the interface, namely, with its domain structure, stabilized by nonmagnetic defects. The latter is responsible for the formation of domains in antiferromagnets and the domains are distributed so that the number of spins in its two sub lattices is not the same[41].

III.2.4. Ferrimagnetic materials:

Ferrimagnetism is a type of permanent magnetism that occurs in solids in which the magnetic fields associated with individual atoms spontaneously align themselves, some parallel, or in the same direction (as in ferromagnetism), and others generally antiparallel, or paired off in opposite directions (as in antiferromagnetism). The magnetic behavior of single crystals of ferrimagnetic materials may be attributed to the parallel alignment; the diluting effect of those atoms in the antiparallel arrangement keeps the magnetic strength of these materials generally less than that of purely ferromagnetic solids such as metallic iron.

III.3. Heusler alloys

III.3.1. Introduction:

Over recent decades there was a significant rise of interest to Heusler alloys due to the their wide range of applications in spintronics. From the standpoint of spintronics, spin polarization of electrons play an important role. Theoretically, such alloys can demonstrate 100% spin polarization and can be used as spin-polarized electron sources along with metal oxides and III–V group semiconductors.[42]The history of Heusler alloys began in 1898, when the German physicist Friedrich Heusler discovered Cu-Mn-Al to be ferromagnetic, although the alloy consists of non-ferromagnetic elements[43, 44]. However, at the present time in such materials, we can observe not only ferromagnetism, but also antiferromagnetism, paramagnetism, diamagnetism, etc. Because of the wide range of properties, these compounds can have the behavior of: semi-metals, semiconductors, superconductors and many others. Today two classes of materials are called Heusler alloys: The semi-Heusler alloys with general formula XYZ and the full-Heusler alloys with X_2YZ. The X and Y elements come from the transition metal group, whereas the Z component is the element of the III-V group. In rare cases, element Y can be a rare earth element, or an alkaline earth metal. Generally, the doubled atom X is located at the beginning of the formula, and the atom of group III-V at the end, as for example the Co_2MnSi.[45, 46]However, there are exceptions where the order of classification follows the scale of electronegativity, for example the element LiCu2Sb[18]. The main combinations of Heusler alloys are presented in (Figure III.1).

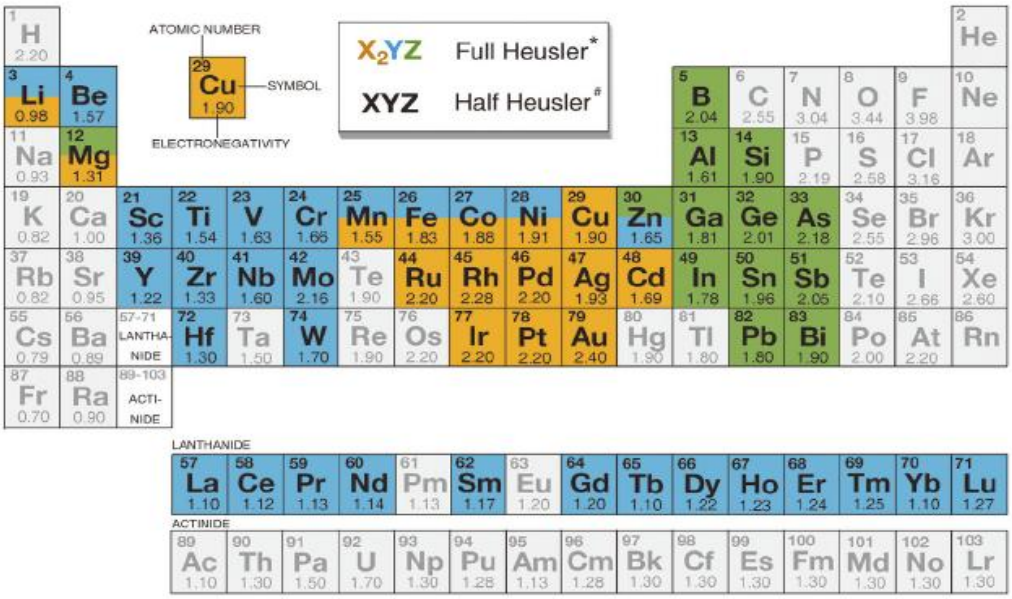

Figure III.1: Periodic table of Heusler compounds

III.3.2. Half-Heusler alloys:

Half-Heusler alloys have the general formula XYZ and crystallize in a non-centro-symmetric cubic structure space group number 216, (F-43m, $\boldsymbol{C1_b}$) that can be derived from the ZnS tetrahedral structure by filling the octahedral sites of the lattice (figure III.2) This typeof semi-Heusler structure can be characterized by the interpenetration of three cubic sub-lattice with centered faces (cfc) The positions occupied are 4a (0, 0, 0), 4b (1/2, 1/2, 1/2), and 4c (1/4, 1/4, 1/4).Three non-equivalent atomic arrangements for this type of structure (C1b) can be associated; the Table presents these different possibilities:The atomic arrangements mentioned above depend on two factors; one is the difference in size between the atoms, while the other is the type of the interatomic interaction.

Table III.1: Different types of occupancy of non-equivalent sites in the $C1_b$ structure.

Les atomes	*X*	*Y*	*Z*
1^{er} *arrangement*	*4a*	*4b*	*4c*
$2^{ème}$ *arrangement*	*4b*	*4c*	*4a*
$3^{ème}$ *arrangement*	*4c*	*4a*	*4b*

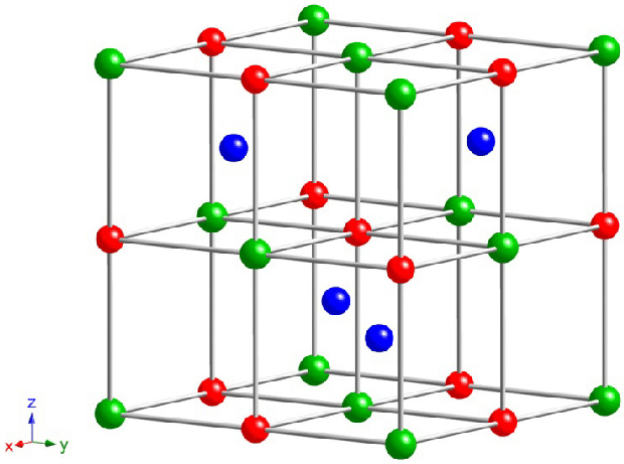

Figure III.2: Crystal structure of a typical Half-Heusler

III.3.3. Full Heusler alloys:

The full Heusler alloys are ternary systems with the composition 2:1:1 represented by the formula X_2YZ. They crystallize in the $L2_1$ structure with space group $Fm\bar{3}m$ (space group number 225) [47]. (Figure III.3) shows the completely ordered $L2_1$- type ordered crystal structure of full Heusler alloys [48]In the $L2_1$ ordered structure, the unit cell consists of four interpenetrating fccsublattices with the positions (0, 0, 0) and (1/2, 1/2, 1/2) for X, (1/4, 1/4, 1/4) for Y and (3/4, 3/4, 3/4). For Z atomsX element is typically the most electronegative transition metal like Co, Cu, Ni or Fe,Y element is the less electronegative transition metal Which is mainly Mn. In some cases, the Y element may also be an alkaline earth metal. Z element is a main group element, such as Ge, Si, Ga, Sn, Sb, Al or In. The characteristics of full Heusler alloys depend strongly on the atomic order.

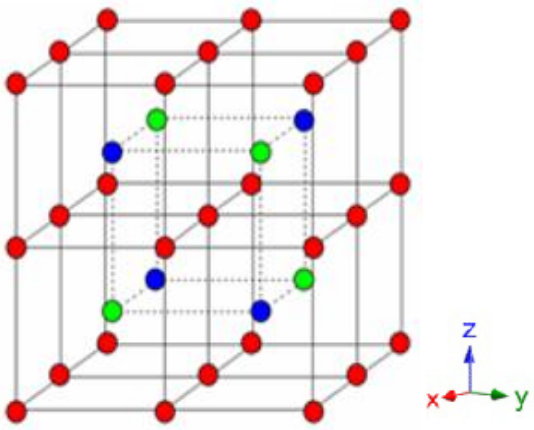

Figure III.3: Crystal structure of a typical F-Heusler.

III.3.4. Quaternary Heusler Compounds:

When one of the two X atoms in X_2YZ compounds (full-Heusler compounds) is substituted by a different transition metal X′ , a quaternary compound with the composition XX′YZ and F 43m symmetry (space group no. 216) is generated. The prototype of this Y -type structure of quaternary Heusler compounds is LiMgPdSn[49, 50].Three possible nonequivalent superstructures based on the different positions of the four atoms exist for this structure type as indicated in(table III.2).

Table 02: Three possible positions of the atoms for the quaternary Heusler alloys XX 'YZ.

	4a (0,0,0)	*4c (1/4,1/4,1/4)*	*4b (1/2,1/2,1/2)*
1erarrangement	*X*	*Z*	*Y*
2èmearrangement	*Z*	*Y*	*X*
3èmearrangement	*Y*	*X*	*Z*

III.4. Heusler Compounds as Half-metallic Ferromagnets:

Half-metallic ferromagnets represent a new class of materials which absorbed a lot of attention considering their possible applications in spintronics (also known as magneto-electronics)[51]. In these materials the spin resolved bands have a special behavior. One of the spin densities (in most cases majority) shows typically a metallic behavior while the other (in most cases minority) is semiconductor. Therefore, the half-metallic ferromagnets exhibit 100% spin polarization at the Fermi energy which is supposed to maximize the efficiency of magneto-electronic devices [52, 53]. Until now a lot of half-metallic ferromagnets are known. Full-Heusler and half Heusler alloys are the most prominent among the half-metallic compoundsHeusler compounds first attracted interest among the scientific community in 1903, when F. Heusler found that the compound Cu2MnAl becomes ferromagnetic, although non of itsconstituent element is ferromagnetic by itself [54]The origin of interest in magnetic properties of the Heusler compounds is the prediction of half-metallic ferromagnetism inMnNiSb by de Groot et al [3]and in Co2MnSn by K¨ubler et al [55]. In many Heusler compounds the total magnetic moment follows a simple electroncounting rule based on the Slater-Pauling behavior .[56]

III.5. Slater-Pauling behavior:

Slater [57] and Pauling [58] independently discovered that the total magnetic moment (M_t) of the 3d elements and their binary alloys can be estimated on the basis of the average

number of valence electrons (Z_t) per atom.Thus, there is a curve, called the Slater-Pauling curve, which represents the variation of the magnetic moment as a function of the total number of valence electrons .Depending on M_t (Z_t), the materials are divided into two classes. The first part of the Slater-Pauling curve, is the area of itinerant magnetism and high number of valence electron ($Z_t \geq 8$). The second part is the area of localized magnetism and low number of valence electron ($Z_t \leq 8$). Iron is located on the borderline between localized and itinerant magnetism.(Figure III.4)

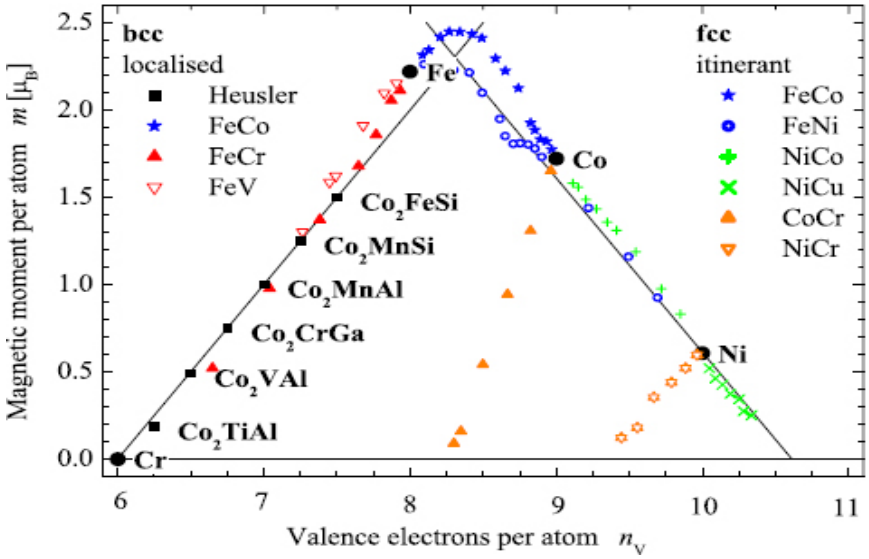

Figure III.4: Slater-Pauling curve for 3d transition metals and some of their alloys.

The total number of valence electrons in the unit cell Z_t is given by the sum of the number of spin–up ($N_\uparrow$) and spin–down ($N_\downarrow$) electrons, while the total moment M_t is given by the difference between them. this is summarized by the relations below :

$$Z_t = N_\uparrow + N_\downarrow \quad \text{(III.3)}$$

$$M_t = N_\uparrow - N_\downarrow \quad \text{(III.4)}$$

$$M_t = Z_t - 2N_\downarrow \quad \text{(III.5)}$$

Slater and Pauling showed that in the case of binary magnetic compounds, when we add one valence electron in the compound this occupies spin-down states only and the total spin magnetic moment decreases by about 1μB [23,24]. Interestingly, a similar behavior can also be found in half-metallic Heusler compounds, where the extra valence electron now occupies spin-up states increasing the total spin magnetic moment by about 1μB. It was shown that in the case of the semi-Heusler compounds such as NiMnSb, the total spin magnetic in the unit cell, Mt, scales,

as a function of the total number of valence electrons Z_t, following the relation: $M_t = Z_t - 18{,}28$ while in the case of the full-Heusler this relation becomes $M_t = Z_t - 24.29$ These Slater-Pauling (SP) rules connect the electronic properties(the appearance of the half-metallic behavior) directly to the magnetic properties (total spin magnetic moments) and thus offer a powerful tool to the study of half-metallic Heusler compounds. It has been shown that also quaternary or half-metallic Heusler compounds obey the SP:

$$M_t = Z_t - 18 \quad \text{(III.6)}$$

$$M_t = Z_t - 24 \quad \text{(III.7)}$$

Chapter IV Results and Discussions

IV.1. Introduction:

In this chapter, we systemically study the structural, electronic, elastic and magnetic properties of CrCoScAl, using wien2k code. We chose CrCoScAl as our field of study, as it has exceptional properties ranging from half-metallicity [59, 60], high Curie temperature [61] to spin gapless semiconducting[62, 63]that have been successfully exploited for technological applications.

IV.2. Calculation details:

All calculations have been carried out using the full-potential linear-augmented plane-wave method (FP-LAPW) in the framework of the density functional theory (DFT) using the generalized gradient approximation of Perdew-Burke-Ernzehof (GGA-PB[64, 65]implemented in WIEN2k package [29, 66], which self-consistently finds the eingenvalues and eingen function of the Kohn-Sham [67] equations for the system. The wave function, charge density and potential have been extended by spherical harmonic functions inside non-overlapping spheres surrounding the atomic sites (muffin-tin spheres) and by a plane-wave basis set in the remaining space of the unit cell (interstitial region).

The RMT * Kmax parameter is chosen to be equal to 8, (Where Kmax is the maximum modulus for the reciprocal lattice vector, and RMT is the average radius of the muffin tin spheres). Table V.1shows the radii of the RMT spheres of the different atoms taken into account during the calculations. The Brillouin zone is integrated with 2000 k-points.

Table IV.1: RMT values (in a.u) for the Cr, Co, Sc, and Al atoms.

Atome	*Cr*	*Co*	*Sc*	*Al*
R_{MT}	*2.300*	*2.400*	*2.2800*	*2.1600*

IV.3. Structural and mechanical properties:

In ab-initio calculation, the most important step is to determine the structural properties of a given system on its ground state, which will later allow us to know other important physical properties. The quaternary Heusler alloys are inter-metallic

compounds with stoichiometric composition XX'YZ, where X, X' and Y are transition metal elements and Z is a III, IV or V group element. These compounds crystallize with cubic structure LiMgPdSb-type denoted as Y-type with an F43m space group [49, 68]. As shown in **Figure (IV.1)a**nd **Table (IV.2)**, three possible nonequivalent superstructures based on the different positions of the X, X' and Y atoms exist for this structural type.

Table IV.2: Different types of structure for CrCoScAl compound.

	$4a$ (0,	$4c$ $(\frac{1}{4},\frac{1}{4},\frac{1}{4})$	$4b$ $(\frac{1}{2},\frac{1}{2},\frac{1}{2})$	$4d$ $(\frac{3}{4},\frac{3}{4},\frac{3}{4})$
Type I	***Sc***	***Co***	***Cr***	***Al***
Type II	***Sc***	***Cr***	***Co***	***Al***
Type III	***Co***	***Sc***	***Cr***	***Al***

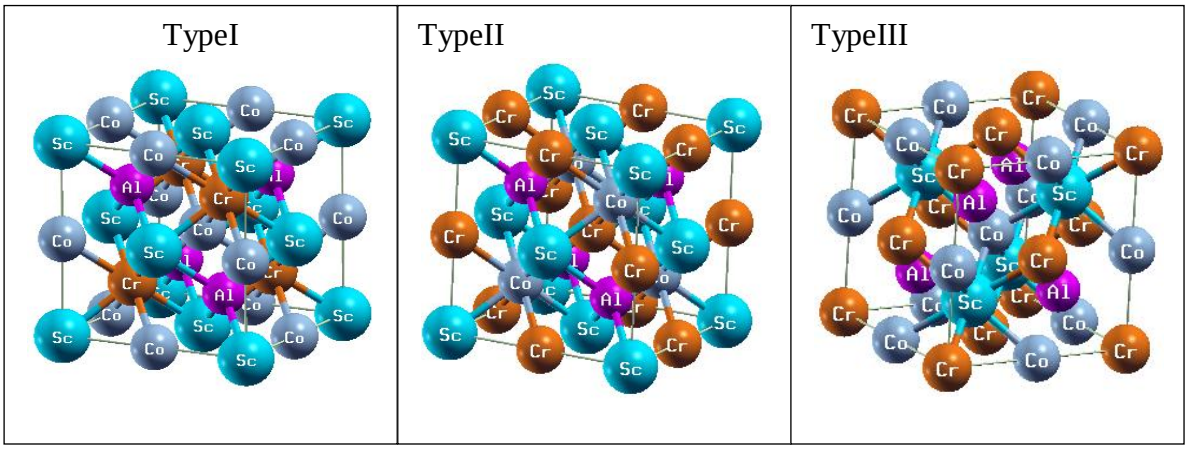

Figure IV.1 Different types of structure for CrCoScAl compound.

In the first step, we calculate the energy versus volume for the three types of quaternary Heusler structures for ferromagnetic (FM) and non-magnetic(NM) phases and we represent them in **Figure (IV-2)**.The calculated total energies within GGA as functions of the volume are fitted with Birch-Murnaghan equation, to obtain the ground state properties**.**

$$E(V) = E_0 + \frac{9V_0B_0}{16}\left\{\left[\left(\frac{V_0}{V}\right)^{2/3} - 1\right]^3 \grave{B}_0 + \left[\left(\frac{V_0}{V}\right)^{2/3} - 1\right]^2 \left[6 - 4\left(\frac{V_0}{V}\right)^{2/3}\right]\right\} \qquad \text{(IV.1)}$$

We observe from these graphs that our compound is more stable in the type III ferromagnetic phase because its corresponding energy is the lowest.

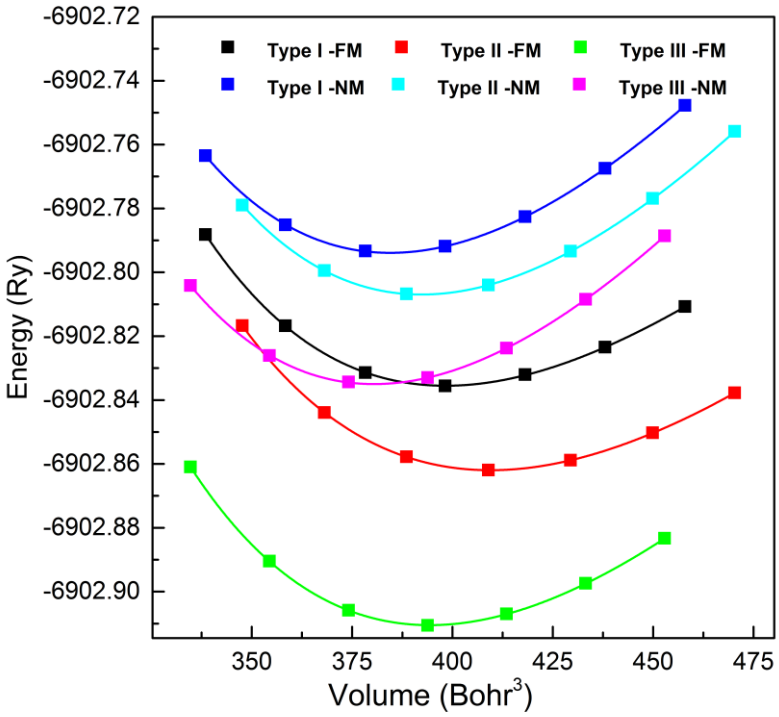

Figure IV.2: Optimization of total energy as a function of volume using the GGA approximation**.**

In **Table (IV.3)**, we report our calculated equilibrium lattice constants, bulk modulus B, its pressure derivative B' and the total energy E_0 in their three different configurations at zero pressure and ambient temperature. While the compressibility modulus is determined by the equation:

$$B = V\frac{\partial^2 E}{\partial V^2} \qquad \text{(IV.2)}$$

Table IV-3: Lattice parameter, cell volume, bulk modulus, its derivative, and total energy.

	a(Bohr)	*V_0*	*B(GPA)*	*$B^{'}$(GPA)*	*E_0*
CrCoScAl	*11.6403*	*394.3091*	*119.1421*	*4.6184*	*-6902.9104*

IV.4. Elastic properties:

In order to confirm the stability of our material, we studied their elastic properties which provide us with information about the rigidity, anisotropy, thermal expansion of the materials and Debye temperature. The elastic behavior of materials

is generally described by models based on a linear elastic behavior law, called Hooke's law. . The calculation of the elastic constants for our alloy is developed recently by Thomas Charpin method implemented inWIEN2k code [69]. In the case of a cubic crystal, the number of elastic constants can be reduced to three independent constants C_{11}, C_{12}et C_{44}.Following certain symmetry considerations, their determination requires the arrangement of the three equations to be solved, created by the application of three different types of deformation.The measurement of elastic constants from total energy is based on the Mehl process, which imposes the conservation of the sample volume under pressure impact[70]. Using Mehl's[71]model, we calculate the modulus (C_{11}, C_{12}) by the orthorhombic deformation tensor in conserved volume:

$$\vec{\varepsilon} = \begin{bmatrix} \delta & 0 & 0 \\ 0 & -\delta & 0 \\ 0 & 0 & \frac{\delta^2}{1-\delta} \end{bmatrix} \quad \text{(IV.3)}$$

Where δ is the applied deformation. The application of this constraint influences the total energy:

$$E(\delta) = E(-\delta) = E(0) + (C_{11} - C_{12})V\delta^2 + o[\delta^4] \quad \text{(IV.4)}$$

With $E(0)$ is the energy of the system taken in the initial state (without constraint) and V is the conserved volume of the primitive cell . From the curve, we will get the following formula:

$$E(\delta) = b\delta^2 + E(0) \quad \text{(IV.5)}$$

b Is the graph's incline coefficient $E = f(\delta)$ (VI.6)

$$C_{11} - C_{12} = \frac{b}{V_0} \quad \text{(IV.7)}$$

To obtain the C_{11} andC_{12}values, we need a second equation given by the module of compressibility for an isotropic cubic crystal by:

$$B = \frac{1}{3}(C_{11} + 2C_{12}) \quad \text{(IV.8)}$$

Finally, to determine the third elastic constant C_{44}, a monoclinic deformation occurs with the conserved volume given by the following expression:

$$\vec{\varepsilon} = \begin{bmatrix} 0 & \frac{\delta}{2} & 0 \\ \frac{\delta}{2} & 0 & 0 \\ 0 & 0 & \frac{\delta^2}{4-\delta^2} \end{bmatrix} after\ diagonalization \quad \vec{\varepsilon} = \begin{bmatrix} \frac{\delta}{2} & 0 & 0 \\ 0 & -\frac{\delta}{2} & 0 \\ 0 & 0 & \frac{\delta^2}{4-\delta^2} \end{bmatrix} \quad \text{(IV.9)}$$

The total energy becomes:

$$E(\delta) = E(-\delta) = E(0) + \frac{1}{2} C_{44} V \delta^2 + o[\delta^4] \quad \text{(IV.10)}$$

And the total energy equation is in the form of:

$$E(\delta) = b\delta^2 + E(0) \quad \textbf{(}\text{IV.11)}$$

By replacing **equation (IV-11)** in **equation (IV-10)**, the elastic constant C_{44} can be defined by the following relation:

$$C_{44} = \frac{2b}{V_0} \quad \text{(IV.12)}$$

Where b is the graph's incline. The stability criteria are defined as follows:

$$C_{11} > 0, C_{44} > 0,\ C_{11} > C_{12}, (C_{11} + 2C_{12}) > 0 \text{ et } C_{12} < B < C_{11} \quad \text{(IV.13)}$$

We may determine very important elastic properties from the elastic constants, such as: Anisotropy A, which for an isotropic crystal is equal to 1 while another value greater than or less than 1 means it is an anisotropic crystal.

$$A = \frac{2C_{44}}{C_{11} - C_{12}} \quad \text{(IV.14)}$$

The shear modulus is determined by measuring the deformation of a solid from applying a force parallel to one surface of a solid, while an opposing force acts on its opposite surface and holds the solid in place[72]:

$$G = \frac{1}{5}(3C_{44} + C_{11} - C_{12}) \quad \text{(IV.15)}$$

The Young modulus E which measures the resistance of the solid to the change of its length:

$$E = \frac{9BG}{3B+G} \quad \text{(IV.16)}$$

Poisson's ratio is the ratio of transverse contraction strain to longitudinal extension strain in the direction of stretching force[73].

$$\nu = \frac{1}{2}(1 - \frac{E}{3B}) \quad \text{(IV.17)}$$

The obtained values, from the elastic constants C_{11}, C_{12},C_{44}, parameters ,*E, G,ν, A* and the ratio *B/G* of our compound are listed in **Tables (IV.4,5).**

Table IV.4: Elastic constants ($\boldsymbol{C_{11}}$, $\boldsymbol{C_{12}}$,$\boldsymbol{C_{44}}$) and Compressibility module B for CrCoScAl compound.

	C_{11}	C_{12}	C_{44}	B
CrCoScAl	204.31	76.799	105.307	119.30

Table IV.5: Young's modulus, Shear modulus G, Poission's coefficient υ, Anisotropy parameter A and B / G ratio for the compound CrCoScAl.

	E	*G*	*ν*	*B/G*	*A*
CrCoScAl	*208.227*	*86.302*	*0,209*	*1.3855*	*1.4895*

From the two tables above, it is clear that the elastic constants are positive and verify the criteria of mechanical stability of cubic crystals**:**

$$C_{11} > 0\ ,C_{44} > 0,\ \ C_{11} > C_{12}\ ,(C_{11} + 2C_{12}) > 0 \text{ et } C_{12} < B < C_{11} \quad \text{(IV.18)}$$

Therefore, our compound is mechanically stable. We can see clearly that the coefficient A is greater than the unit, so we can assume that our compound is an anisotropic material. We can see that the B / G ratio is greater than the critical value 1.75 which divides ductile / brittle behaviors (/ brittle <1.75< ductile), which allows us to classify our compound as a brittl material.

IV.5. Debye temperature:

To better understand the effect of atomic vibrations in a solid, it is also interesting to determine the thermal characteristics of materials using one of the most important parameters which is the Debye temperature θ_D.The Debye temperature was calculated using the average speed of sound by the following equation:

$$\theta_D = \frac{h}{k}\left[\frac{3n}{4\pi}\left(\frac{N_A \rho}{M}\right)\right]^{\frac{1}{3}} v_m \quad \text{(IV.19)}$$

whereh is the Planck constant, k the Boltzmann constant, N_A the Avogadro number, n the number of atoms, M the molecular, the density$\rho = \left(\frac{M}{V}\right)$ .As a general rule, a high

value of θ_D implies a high thermal conductivity and a high fusion temperature and particularly a hard material. We can easily calculate the average speed of sound using by the equation:

$$v_m = \left[\frac{1}{3}\left(\frac{2}{{v_t}^3} + \frac{1}{{v_l}^3}\right)\right]^{\frac{1}{3}} \quad \text{(IV.20)}$$

Where v_t and v_l are the longitudinal and transverse speeds respectively, and are expressed by Navier's equations [74]:

$$v_l = \sqrt{\frac{3B+4G}{3\rho}} \quad \text{and} \quad v_t = v\sqrt{\frac{G}{\rho}} \quad \text{(IV.21)}$$

Table (IV.6) presents the results obtained for the material CrCoScAl. It seems that our material has a high Debye temperature, which indicates that it can have a high thermal conductivity.

Table IV.6: Longitudinal v_l, transverse v_t and average speeds of sound v_m in m/s, Debye temperature θ_D in K.

$v_l(m/s)$	$v_t(m/s)$	$v_m(m/s)$	$\theta_D(K)$
5689.68	***2986.93***	***3340.5***	***387.973***

IV.6. Electronic properties

IV.6.1. Band structures

The spin polarized band structures of CrCoScAl quaternary Heusler compound were calculated along the high symmetry path of the first Brillouin zone at the equilibrium lattice constants. It was found that CrCoScAl compound exhibits a half-metallic behavior as shown in **Figure (IV.3)**. The bands of spin-up cross the Fermi energy level, which correspond to a metallic behavior. However, the spin-dn band structure shows a semiconducting behavior with an indirect band gap of 0.55eV, where the valence band maximum (VBM) and the conduction band minimum (CBM) are located at Γ and L high symmetry points, respectively. Although this material exhibits a metallic behavior for the spin-up channel and a semiconducting behavior in the spin-dn channel.

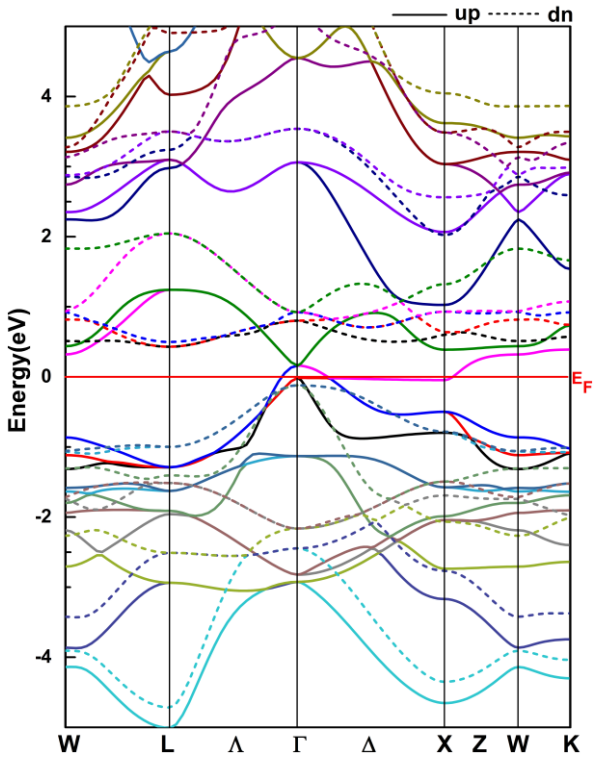

Figure IV.3: Spin-up and spin-down band structure for CrCoScAl compound for the first Brillouin zone.

IV.6.2.Density of States

Density state is generally used to understand the electronic structure of a compound in detail. Taking into account the spin polarization (spins up and down) , The total and partial densities of states for CrCoScAl alloy in the ferromagnetic phase are calculated by GGA approximation at its equilibrium state. Its curves can be seen in **Figure (IV.4).**

From **Figure (IV.4)**, it is clear that the majority-spin (spin-up) have a metallic character, while appearance of the gap at Fermi level in the case of minority spins, which confirms the half-metallicity behavior. The contribution of electronic states differs from one atom to another, Around the Fermi level. Atoms (Cr and Co) show major contributions to the total density of states, while Sc and Al atoms exhibit negligible contributions.

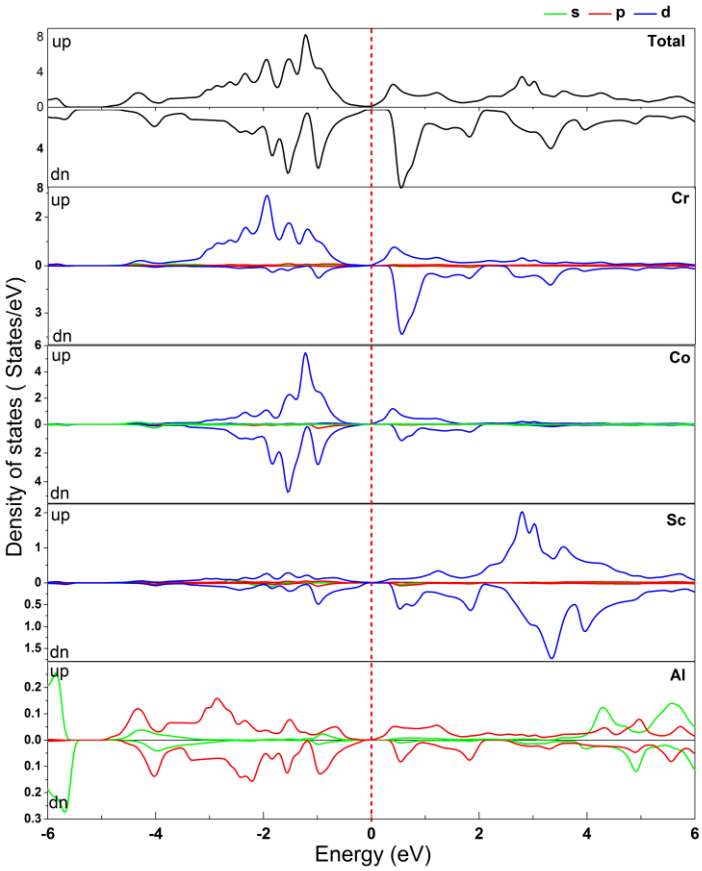

Figure IV.4: Calculated total and partial densities of states for CrCoScAl by GGA approximation

IV.7. Magnetic properties:

This subsection presents the magnetic properties of CrSoScAl quaternary Heusler compounds. The local and total magnetic moment calculated under the constant equilibrium lattice is given in **Table(IV.7)**.CrSoScAl compound shows a ferromagnetic material with total magnetic moment of$2\mu_B$.We observe that the Cr atom makes a greater contribution to the total magnetic moment than that of Co atom, while the Cu presents negligible contributions. Though the importance of the local magnetic moment is negligible for metalloid atoms, it affects the value of the total magnetic moment. Slater-Pauling rule could indicate the half-metallicity of material using its total magnetic moment, where the integer value of total magnetic moment refers to half-metallic behavior. The Slater-Pauling rule of CrSoScAl compound is equated with the following[57, 58]:

$$M_t = Z_t - 18 \qquad \text{(IV.22)}$$

$$Z_t = 20 \quad so \quad M_t = 20 - 18 = 2\mu_B \qquad \text{(IV.23)}$$

Table IV.7: *Local and total magnetic moments of CrCoScAl.*

	M_{Cr}	M_{Co}	M_{Sc}	M_{Al}	M_{int}	M_{Tot}	$P \times 100$
CrCoScAl	*1,24527*	*0,23959*	*0,02424*	*0,00105*	*0,49006*	*2,00021*	*100%*

IV.8. Spin polarization:

The electronic spin polarization of the studied compound is calculated using the following relation:

$$P(E_f) = \frac{\rho\uparrow(E_f) - \rho\downarrow(E_f)}{\rho\uparrow(E_f) + \rho\downarrow(E_f)} \times 100 \qquad \text{(IV.24)}$$

With$\rho \uparrow (E_f)$ and $\rho \downarrow (E_f)$ are the values of majority and minoritydensities of states at Fermi level E_F. Note from the results listed in **Table (IV.7)** that the spin polarization of our compound is 100%. This result, as well as that of the total magnetic moment, confirms the half-metallic character of our compound.

References:

1. Bouabça, A., et al., *Half-metallic completely compensated ferrimagnets in Cr doped BaP*. Chinese Journal of Physics, 2016. **54**(4): p. 489-494.
2. Heusler, F., *Über magnetische manganlegierungen Verh.* Dtsch. Phys. Ges, 1903. **5**: p. 219.
3. De Groot, R., et al., *New class of materials: half-metallic ferromagnets.* Physical Review Letters, 1983. **50**(25): p. 2024.
4. Aguayo, A. and G. Murrieta, *Density functional study of the half-metallic ferromagnetism in Co-based Heusler alloys Co2MSn (M= Ti, Zr, Hf) using LSDA and GGA.* Journal of Magnetism and Magnetic Materials, 2011. **323**(23): p. 3013-3017.
5. Katsnelson, M., et al., *Half-metallic ferromagnets: From band structure to many-body effects.* Reviews of Modern Physics, 2008. **80**(2): p. 315.
6. Wolf, S., et al., *Spintronics: a spin-based electronics vision for the future.* science, 2001. **294**(5546): p. 1488-1495.
7. Şaşıoğlu, E., et al., *Exchange interactions and temperature dependence of magnetization in half-metallic Heusler alloys.* Physical review B, 2005. **72**(18): p. 184415.
8. Wurmehl, S., et al., *Investigation of Co 2 Fe Si: The Heusler compound with highest Curie temperature and magnetic moment.* Applied physics letters, 2006. **88**(3): p. 032503.
9. Galanakis, I., *Surface properties of the half-and full-Heusler alloys.* Journal of Physics: Condensed Matter, 2002. **14**(25): p. 6329.
10. Thomas, L.H. *The calculation of atomic fields*. in *Mathematical Proceedings of the Cambridge Philosophical Society*. 1927. Cambridge University Press.
11. Fermi, E., *Statistical method to determine some properties of atoms.* Rend. Accad. Naz. Lincei, 1927. **6**(602-607): p. 5.
12. Hartree, D.R. *The wave mechanics of an atom with a non-Coulomb central field. Part I. Theory and methods*. in *Mathematical Proceedings of the Cambridge Philosophical Society*. 1928. Cambridge University Press.
13. Dirac, P.A.M., *Quantum mechanics of many-electron systems.* Proceedings of the Royal Society of London. Series A, Containing Papers of a Mathematical and Physical Character, 1929. **123**(792): p. 714-733.
14. Dirac, P.A. *Note on exchange phenomena in the Thomas atom*. in *Mathematical Proceedings of the Cambridge Philosophical Society*. 1930. Cambridge University Press.
15. Fock, V., *Näherungsmethode zur Lösung des quantenmechanischen Mehrkörperproblems.* Zeitschrift für Physik, 1930. **61**(1-2): p. 126-148.
16. Schrödinger, E., *An undulatory theory of the mechanics of atoms and molecules.* Physical review, 1926. **28**(6): p. 1049.
17. Born, M. and R. Oppenheimer, *Zur quantentheorie der molekeln.* Annalen der physik, 1927. **389**(20): p. 457-484.
18. Giustino, F., *Materials modelling using density functional theory: properties and predictions*2014: Oxford University Press.
19. Slater, J.C., *Wave functions in a periodic potential.* Physical review, 1937. **51**(10): p. 846.
20. Heisenberg, W., *Über den anschaulichen Inhalt der quantentheoretischen Kinematik und Mechanik*, in *Original Scientific Papers Wissenschaftliche Originalarbeiten*1985, Springer. p. 478-504.
21. Nagy, A., *Relativistic density-functional theory for ensembles of excited states.* Physical Review A, 1994. **49**(4): p. 3074.
22. Hedin, L. and S. Lundqvist, *Effects of electron-electron and electron-phonon interactions on the one-electron states of solids*, in *Solid state physics*1970, Elsevier. p. 1-181.
23. Cuevas-Saavedra, R. and V.N. Staroverov, *Exact expressions for the Kohn–Sham exchange-correlation potential in terms of wave-function-based quantities.* Molecular Physics, 2016. **114**(7-8): p. 1050-1058.
24. Perdew, J., K. Burke, and M. Ernzerhof, *Perdew, burke, and ernzerhof reply.* Physical Review Letters, 1998. **80**(4): p. 891.
25. Slater, J., *Energy band calculations by the augmented plane wave method*, in *Advances in quantum chemistry*1964, Elsevier. p. 35-58.
26. Koelling, D. and G. Arbman, *Use of energy derivative of the radial solution in an augmented plane wave method: application to copper.* Journal of Physics F: Metal Physics, 1975. **5**(11): p. 2041.
27. Andersen, O.K., *Linear methods in band theory.* Physical review B, 1975. **12**(8): p. 3060.

28. Sjöstedt, E., L. Nordström, and D. Singh, *An alternative way of linearizing the augmented plane-wave method.* Solid state communications, 2000. **114**(1): p. 15-20.
29. Madsen, G.K., et al., *Efficient linearization of the augmented plane-wave method.* Physical review B, 2001. **64**(19): p. 195134.
30. Kohn, W. and L.J. Sham, *Self-consistent equations including exchange and correlation effects.* Physical review, 1965. **140**(4A): p. A1133.
31. Vosko, S.H., L. Wilk, and M. Nusair, *Accurate spin-dependent electron liquid correlation energies for local spin density calculations: a critical analysis.* Canadian Journal of physics, 1980. **58**(8): p. 1200-1211.
32. Godby, R., M. Schlüter, and L. Sham, *Accurate exchange-correlation potential for silicon and its discontinuity on addition of an electron.* Physical Review Letters, 1986. **56**(22): p. 2415.
33. Becke, A.D., *Density-functional exchange-energy approximation with correct asymptotic behavior.* Physical Review A, 1988. **38**(6): p. 3098.
34. Perdew, J.P., et al., *Erratum: Atoms, molecules, solids, and surfaces: Applications of the generalized gradient approximation for exchange and correlation.* Physical review B, 1993. **48**(7): p. 4978.
35. Perdew, J.P., K. Burke, and M. Ernzerhof, *Generalized gradient approximation made simple.* Physical Review Letters, 1996. **77**(18): p. 3865.
36. Anisimov, V.I., J. Zaanen, and O.K. Andersen, *Band theory and Mott insulators: Hubbard U instead of Stoner I.* Physical review B, 1991. **44**(3): p. 943.
37. Vulliermet, N., *Investigation théorique du mécanisme de physisorption: application d'une méthode de partition fondée sur la fonctionnelle de la densité*, 2000, University of Geneva.
38. Tikadzumi, S., *Physics of ferromagnetism.* Magnetic Characteristics and Practical Applications, 1983.
39. Madelung, O., *Physics of III-V compounds*1964: J. Wiley.
40. Krinchik, G., *Physics of magnetic effects.* Moscow State Univ., Moscow, 1976.
41. Hurd, C., *Varieties of magnetic order in solids.* Contemporary Physics, 1982. **23**(5): p. 469-493.
42. Bainsla, L. and K. Suresh, *Equiatomic quaternary Heusler alloys: A material perspective for spintronic applications.* Applied Physics Reviews, 2016. **3**(3): p. 031101.
43. Heusler, F., W. Starck, and E. Haupt, *Verhandlungen der deutschen physikalischen gesellschaft.* Verh. DPG, 1903. **5**: p. 220.
44. Heusler, F., *Mangan-aluminium-kupferlegierungen.* Verh. DPG, 1903. **5**: p. 219.
45. BENYETTOU, S., *Calcul de premier principe de quelques propriétés physiques de quelques alliages semi-conducteurs*, 2016, Université Mohamed Khider-Biskra.
46. De Vito, D.A., *Modélisation de réactions chimiques par des méthodes de chimie quantique: adsorption du méthanol sur une surface de γ-alumine: échange de molécules d'eau dans des complexes hexaaquo de rhodium (III) et iridium (III)*, 2003, University of Geneva.
47. Heusler, O., *Kristallstruktur und Ferromagnetismus der Mangan- Aluminium- Kupferlegierungen.* Annalen der physik, 1934. **411**(2): p. 155-201.
48. Yıldırım, S., *Nanoyapıdaki Ni50Mn34-Xcuxın16 (X= 1.3, 1.5) Heusler Alaşımlarının Manyetik Özelliklerinin İncelenmesi.* 2014.
49. Drews, J., U. Eberz, and H.-U. Schuster, *Optische Untersuchungen an farbigen Intermetallischen phasen.* Journal of the Less Common Metals, 1986. **116**(1): p. 271-278.
50. Bacon, G. and J. Plant, *Chemical ordering in Heusler alloys with the general formula A2BC or ABC.* Journal of Physics F: Metal Physics, 1971. **1**(4): p. 524.
51. Žutić, I., J. Fabian, and S.D. Sarma, *Spintronics: Fundamentals and applications.* Reviews of Modern Physics, 2004. **76**(2): p. 323.
52. De Boeck, J., et al., *Technology and materials issues in semiconductor-based magnetoelectronics.* Semiconductor Science and Technology, 2002. **17**(4): p. 342.
53. Galanakis, I., *Orbital magnetism in the half-metallic Heusler alloys.* Physical review B, 2005. **71**(1): p. 012413.
54. Heusler, F., *Über magnetische manganlegierungen.* Verhandlungen der Deutschen Physikalischen Gesellschaft, 1903. **5**: p. 219.
55. Kübler, J., A. William, and C. Sommers, *Formation and coupling of magnetic moments in Heusler alloys.* Physical review B, 1983. **28**(4): p. 1745.
56. Fecher, G.H., et al. *STATE OF Co AND Mn IN HALF-METALLIC FERROMAGNET Co 2 MnSi EXPLORED BY MAGNETIC CIRCULAR DICHROISM IN HARD X-RAY*

PHOTOELECTRON EMISSION AND SOFT X-RAY ABSORPTION SPECTROSCOPIES. in *Spin*. 2014. World Scientific.
57. Slater, J.C., *The ferromagnetism of nickel. II. Temperature effects.* Physical Review, 1936. **49**(12): p. 931.
58. Pauling, L., *The nature of the interatomic forces in metals.* Physical Review, 1938. **54**(11): p. 899.
59. Alijani, V., et al., *Electronic, structural, and magnetic properties of the half-metallic ferromagnetic quaternary Heusler compounds CoFeMn Z (Z= Al, Ga, Si, Ge).* Physical review B, 2011. **84**(22): p. 224416.
60. Alijani, V., et al., *Quaternary half-metallic Heusler ferromagnets for spintronics applications.* Physical review B, 2011. **83**(18): p. 184428.
61. Bainsla, L., et al., *CoRuFeX (X= Si and Ge) Heusler alloys: High TC materials for spintronic applications.* Journal of Alloys and Compounds, 2015. **651**: p. 631-635.
62. Bainsla, L., et al., *Origin of spin gapless semiconductor behavior in CoFeCrGa: Theory and Experiment.* Physical review B, 2015. **92**(4): p. 045201.
63. Xu, G., et al., *A new spin gapless semiconductors family: Quaternary Heusler compounds.* EPL (Europhysics Letters), 2013. **102**(1): p. 17007.
64. Perdew, J.P., K. Burke, and M. Ernzerhof, *Perdew, burke, and ernzerhof reply.* Physical Review Letters, 1998. **80**(4): p. 891.
65. Zhao, Y., N.E. Schultz, and D.G. Truhlar, *Exchange-correlation functional with broad accuracy for metallic and nonmetallic compounds, kinetics, and noncovalent interactions*, 2005, American Institute of Physics.
66. Blaha, P., et al., *wien2k.*An augmented plane wave+ local orbitals program for calculating crystal properties, 2001.
67. Bérces, A., et al., *An implementation of the coupled perturbed Kohn-Sham equations: perturbation due to nuclear displacements.* Computer physics communications, 1997. **100**(3): p. 247-262.
68. Dai, X., et al., *New quarternary half metallic material CoFeMnSi.* Journal of Applied Physics, 2009. **105**(7): p. 07E901.
69. Khenata, R., et al., *Full-potential calculations of structural, elastic and electronic properties of MgAl2O4 and ZnAl2O4 compounds.* Physics Letters A, 2005. **344**(2-4): p. 271-279.
70. Nye, J.F., *Physical properties of crystals: their representation by tensors and matrices*1985: Oxford university press.
71. Hamza, A., *CONTRIBUTION A L'ÉTUDE DES PROPRIÉTÉS PHYSICOCHIMIQUES DES ALLIAGES D'HEUSLER*, 2015.
72. Reuss, A., *Calculation of the flow limits of mixed crystals on the basis of the plasticity of monocrystals.* Z. Angew. Math. Mech, 1929. **9**: p. 49-58.
73. Voigt, W., *Lehrbuch der Kristallphysik, edited by: Teubner.* Leipzig (1929.
74. Anderson, O.L., *A simplified method for calculating the Debye temperature from elastic constants.* Journal of Physics and Chemistry of Solids, 1963. **24**(7): p. 909-917.

General conclusion and Outlook

General conclusion

In this dissertation, the structural, elastic, electronic, and magnetic properties of quaternary Heusler alloys CrCoScAl are studied with an effort to have a good candidate for spintronic, using first-principles calculations. The density functional theory (DFT) based Full Potential Augmented Plane Wave (FPLAPW) method, as implemented in WIEN2k package, has been used for this study. The generalized gradient approximation (GGA) was used to construct the exchange-correlation potentials.

The results obtained according to our calculation are as follows:

Structural properties:

The most important step is to determine the structural properties of a given system on its ground state. The quaternary Heusler alloy CrCoScAl can have three different types of structures, according to our calculations , this compound is stable in the ferromagnetic phase type-III, which makes it possible to evaluate the corresponding equilibrium parameters, such as, the lattice constant , the volume V_0, the compressibility module B and its first derivative.

Elastic properties

The calculation of the elastic constants confirms the mechanical stability of the compound the coefficient A is greater than the unit, which allows us to say that it is an anisotropic material. The B / G ratio is greater than the critical value 1.75 which divides ductile / brittle behaviors (/ brittle <1.75< ductile), That lets us to classify our compound as a ductile material.

Electronic and magnetic properties

The electronic structure of CrCoScAl compounds exhibit a metallic behavior for the spin-up channel and a semiconducting behavior in the spin-dn channel within direct band gaps of 0.55 eV. CrCoScAl's total magnetic moment is found to be 2.0 l an integer value that is exactly in keeping with the Slater – Pauling rule, in which Cr atom shows a greater contribution. The compound CrCoScAl exhibited a semi-metallic activity with 100% spin polarization.

Outlook

Our research needs to be a starting point for more complex and additional studies in ever more complicated structures. It might be interesting to pursue investigations on the following points:

- Carry out experimental work in order to compare it with the results obtained.
- Study other properties such as the thermodynamic properties.
- Do other coding studies such as Siesta, VASP.

Abstract

The structural, elastic, electronic and magnetic properties of quaternary Heusler alloys CrCoScAl are investigated using augmented plane wave method(FP-LAPW),based on density functional theory, implemented in wien2k code. The stability of the structure has been checked for different site occupations. Type III is The stable structure, it is again confirmed using stability conditions governed by three independent elastic constants (C_{ij}). The electronic structure of CrCoScAl compounds exhibits a metallic behavior for the spin-up channel and a semiconducting behavior in the spin-dn channel with band gap of 0.55 eV. The total spin magnetic moment of CrCoScAl is found to be 2.0 l an integer value which is in accordance with the Slater–Pauling rule exactly. The CrCoScAl compound showed a half-metallic behavior with 100% spin polarization. These characters allow it to be a good candidate for spintronic applications.

Résumé

Les propriétés structurelles, élastiques, électroniques et magnétiques du composé Heusler quaternaire CrCoScAl ont été calculées par la méthode des ondes planes augmentées (FP-LAPW) qui se base sur la théorie de la fonctionnelle de la densité (DFT) en utilisant le code Wien2K. La stabilité du matériau a été vérifiée pour différentes types de structure. Type III est la structure la plus stable, qui a confirmée à nouveau à l'aide de conditions de stabilité régies par trois constantes élastiques indépendantes (C_{ij}). Après l'étude des propriétés électroniques, nous avons constaté que ce composé présente un comportement métallique pour spin-upet un comportement semi-conducteur dans le cas de spin-dn avec une bande interdite de 0.55eV. Le moment magnétique calculé est $2\mu_B$, il est en bon accord avec la règle de Slater-Pauling. Le composé CrCoScAl a montré un comportement semi-métallique avec une polarisation de spin de 100%. Ces caractères permis le composé d'être un bon candidat pour les applications spintroniques.

ملخص

تم دراسة الخصائص , البنيوية ,الميكانيكية, الالكترونية المغناطيسية لمركب رباعي هسلر CrCoScAl باستخدام طريقة الامواج المستوية المتزايدة خطيا (FP-LAPW) في اطار نظرية دالية الكثافة (DFT) باستعمال برنامج *WIEN2K*.تم التحقق من استقرار المركب من اجل ثلاث بنيات , الثالثة اكثر استقرارا . ثم تأكيد النتيجة السابقة عن طريق حساب ثوابت المرونة (C_{ij}) . الخصائص الالكترونية و المغناطيسية تم مناقشتها أيضا تبعا للدراسة هيكل الفرقة و من كثافة الحالة هذا المركب يحمل فجوة في حالة الأقليات وعزمه المغناطيسي في اتفاق مع قاعدة سلاتر بولينغ $2\mu_B$، أظهر مركب l CrCoScAl سلوكًا نصف معدني مع استقطاب دوران 100٪. هذه السمات تسمح للمركب أن يكون مرشحًا جيدًا للتطبيقاتspintronic.